A Nanoscale Electromechanical Contact Switch for Logic Applications

C. C. Huang [*] and K. L. Ekinci [**]

[*] Electrical and Computer Engineering, Boston University, Boston MA 02215,jchuang@bu.edu
[**] Aerospace and Mechanical Engineering, Boston University, Boston MA 02215,ekinci@bu.edu

ABSTRACT

Here, we describe the operation of a nano-electro-mechanical contact switch. The switch design relies on a sharp contact tip integrated to a compliant nanomechanical beam. When the beam is actuated electrostatically, the tip establishes intimate electrical contact between two electrodes. A preliminary contact switch was fabricated on a Si_3N_4 membrane using optical lithography, electron beam lithography and reactive ion etching. Its quasi-static operation was subsequently demonstrated.

Keywords: nano-electro-mechanical systems, nano-electro-mechanical switch, mechanical logic

1 INTRODUCTION

Recent efforts to scale micro-electro-mechanical systems (MEMS) [1] down into the nanometer scales[i] have created *integiable* nanomechanical structures with *extremely high resonance frequencies* — approaching the pace of semiconductor electronic devices. These nano-electro-mechanical systems (NEMS) come with extremely high resonance frequencies, diminished active masses, tolerable force constants and high quality (Q) factors of resonance. These attributes collectively make NEMS suitable for a multitude of technological and scientific applications.

Here, we demonstrate the operation of a NEMS contact switch — intended for use in electromechanical logic applications. The switch offers such prospects as ultra-fast, ultra-low power operation. In this domain of reduced length scales, however, there are unique physical phenomena that challenge the operation of the switch. For this work, we have considered various physical processes that would effect the switch operation and designed an operable structure. Our design is based on a nanoscale contact between a suspended high frequency resonator and a cathode electrode. The device was fabricated on a Si_3N_4 membrane and was tested in the quasi-static (low-frequency) operation mode. Our preliminary results indicate that contact resistances in the "*on*" state greatly are higher than our estimations.

2 DEVICE FABRICATION

Now, we turn to a detailed description of the device fabrication procedure.

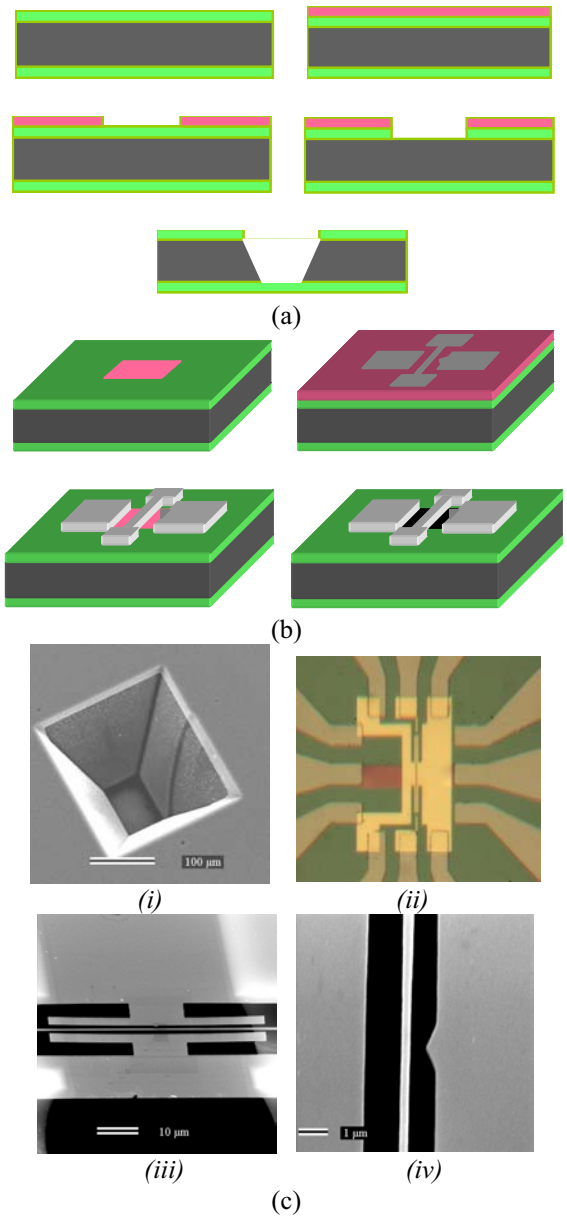

Fig. 1 The device is fabricated by a"top-down" fabrication approach. (a) First, a suspended membrane of Si_3N_4 is fabricated. (b) A contact NEMS switch is nanomachined atop the membrane. (c) *(i)* The back side of the completed membrane, *(ii)* top view of the completed device, *(iii)* and *(iv)* scanning electron micrograph of the switch and contact tip.

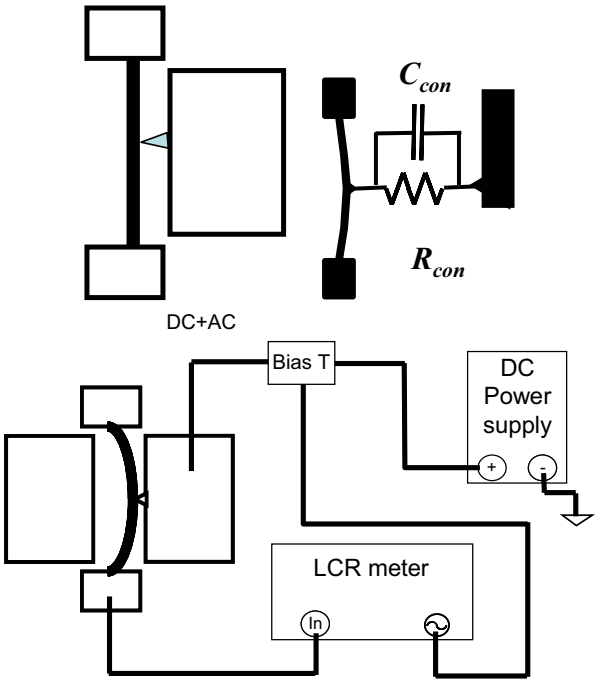

Fig. 2: (a) A schematic of the NEM switch. (b) An equivalent circuit for the switch on contact. (c) The setup employed to measure the contact resistance and capacitance.

The fabrication process has two main steps: manufacturing the suspended silicon nitride (Si_3N_4) membrane, and nanomachining the switch structure atop the membrane.

The membrane fabrication procedure is illustrated in Figure 1 (a). Initially, a silicon (100) wafer of thickness 125 micron is coated on both sides with 125-nm thick silicon nitride using an LPCVD process. Photolithography is then used to pattern a square into the backside of the wafer. Next, reactive ion etching (RIE) with He and SF_6 gases is used to open the nitride layer, exposing the silicon sacrificial layer. A potassium hydroxide (KOH) wet etch is used to dissolve the silicon preferentially in the (100) direction at ~57° angle to the (111) plane. The etch terminates at the Si_3N_4 device layer. The final result of this primary process is a 70 μm x 125 μm Si_3N_4 membrane, clamped at its boundaries.

The device fabrication procedure is illustrated in Figure 1 (b). Fabrication begins on the membrane by defining large area contact pads by optical lithography. A 60 nm-thick layer of Cr is then evaporated and, subsequently, standard liftoff is carried out with acetone. Samples are then coated with a bi-layer PMMA (polymethyl methacrylate) resist prior to patterning by electron beam lithography. After resist exposure and development, 5 nm of Cr and 70 nm of Au are evaporated on the samples, followed by lift-off in acetone. After lift-off, the membrane is removed by using RIE, again. Finally, we use plasma of He and SF_6 at a pressure of 250 mTorr with respective flow rates of 21 sccm and 13 sccm, and a microwave power of 100 W — to suspend the structure. The completed switch structure is shown in Fig. 1(c).

3 DEVICE CONCEPT

A NEMS contact switch thus fabricated is shown in Figure 1 (c). The switch has two electrical terminals: the first terminal is connected to the central nanomechanical beam structure; the second, side electrode is used for actuation as well as detection as shown in Figure 2 (a). The center of the beam displaces in-plane and accomplishes mechanical and electrical contact with the side electrode as shown in Figure 2 (b).

The actuation is realized by using electrostatic forces, *i.e.* by applying a voltage, V_{DC}, to the side electrode. In this scheme, the switch body is kept at electrical ground; the conductance and capacitance through the contact between the nanomechanical beam and the side electrode is measured using a lock-in technique as shown schematically in Figure 2 (c).

To clearly characterize the operation principle of the switch, one needs to compare several competing forces: the *electrostatic* actuation force, the *elastic* restoring force and the *stiction* forces arising from mechanical contact. When the actuation voltage is applied, the structure experiences an attractive electrostatic force towards the side electrode given by

$$F_{es} = \frac{1}{2}\frac{\partial C}{\partial x}V_{DC}^2 \approx \frac{1}{2}\frac{C}{(D-x)}V_{DC}^2 \qquad (1)$$

where C is the capacitance between the beam and the side electrode, D is the initial separation between the beam and the side electrode and x is the displacement of the center of the beam. When the beam bends towards the side electrode, there an elastic restoring force acts upon it given by

$$F_r = -k_{eff}x\,. \qquad (2)$$

Here, $k_{eff} = 32Etw^3/l^3$ is the effective stiffness of the doubly-clamped beam with Young's modulus, E, and dimensions $l \times t \times w$. The actuation force will move the beam until it is equaled by the elastic restoring force of the flexing beam. Using this concept, one can obtain an estimate for the maximum displacement, $x_{\max}$, of the center of the beam.

Upon release of the switch voltage, the elastic restoring force, $F_r \approx -\kappa_{eff}x_{\max}$ must bring the switch back to its original position to create an open circuit. Given that the beam and the side electrode are in physical contact, one must consider the attractive (stiction) forces between the two surfaces. Van der Waals interactions between the atoms (molecules) of the two surfaces can give rise to significant attractive forces, F_{vdW}, at small separations.

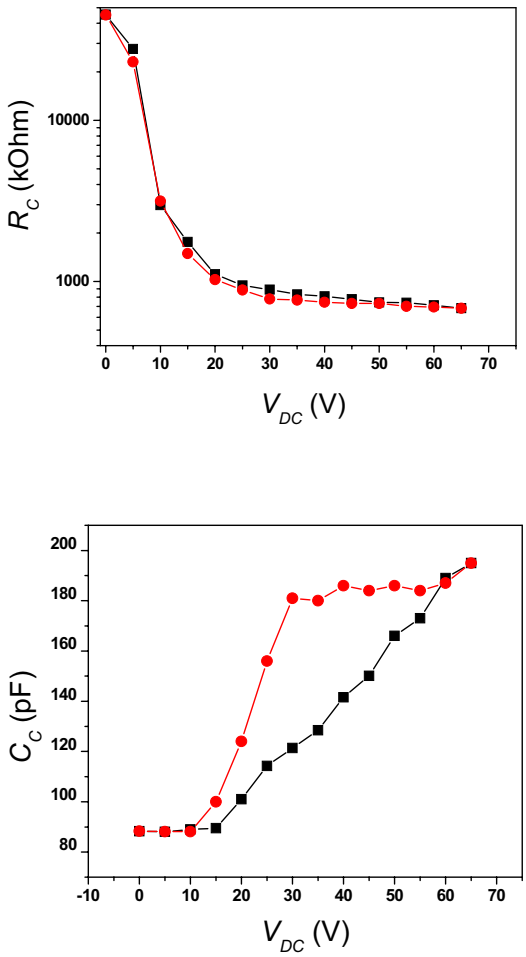

Figure 3: (a) The contact resistance as a function of the actuation voltage. (b) The capacitance as a function of the actuation voltage. The (■) are for increasing voltage values.

Especially in small systems — where surface to volume ratios are large — such short range forces can dominate the system behavior [6, 7].

We have designed our switch with these considerations in mind. The switch structure shown in Figure 1 (c), for instance, has $k_{eff} \approx 0.008$ N/m. The separation between the side electrode and the beam is 500 nm, giving sufficient actuation force at V_{DC}~50 V. The contact radius can be estimated as r~100 nm, giving rise to negligible stiction forces.

4 RESULTS AND ANALYSIS

We now turn to a discussion of our measurements. In these measurements, the contact impedances are measured at a frequency of 1 kHz using a rms amplitude of 50mV.

The contact resistance, R_C, of the switch as a function of the actuation voltage, V_{DC}, is presented in Figure 3 (a). The measurements are taken for increasing and decreasing V_{DC} values. R_C appears to drop precipitously for V_{DC} <10 V. With increasing V_{DC}, R_C saturates around 800 kΩ. R_C displays hysteretic behavior with increasing and decreasing V_{DC} values.

The capacitance of the contact as a function of V_{DC}, is presented in Figure 3 (b). The capacitance, C_C, of the junction appears to increase as expected from the simple expression

$$C_C = \frac{\varepsilon_r \varepsilon_0 A}{(D - x)} \tag{5}$$

C_C also exhibits hysteretic behavior.

We believe that the hysterisis in R_C and C_C, are caused by the stiction phenomenon in the junction.

5 CONCLUSION

In conclusion, a nanomechanical contact switch was fabricated and tested in this work. We have characterized the quasi-static behavior of the switch. The switch displays higher contact resistance than expected. In future work, we will characterize the dynamic behavior of the switch.

REFERENCES

[1] Roukes, M. L. "Nanoelectromechanical systems face the future." *Physics World* **14**, 25-31 (2001).

[2] A. Erbe, R. H. Blick, A. Tilke, A. Kriele, and J. P. Kotthaus, "A mechanically flexible tunneling contact operating at radio frequencies" Appl. Phys. Lett. 73, 3751 (1998)

[3] P. G. Datskos, T. Thundat, "Nanocantiliever Signal Transduction by Electron Transfer" J. Nanosci. Nanotech. 2002, Vol.2, 369 (2002)

[4] W. H. The, J. K. Luo, M. R. Graham, A. Pavlov, C. G. Smith, "Switching characteristics of electrostatically actuated miniaturized micromechanical metallic cantilevers" J. Vac. Sci. Technol. B 21(6), (2003)

[5] E. Buks, M. L. Roukes, "Stiction, adhesion energy, and Casimir effect in micromechanical systems" Phy. Rev. B, Vol.63, 033402 (2001)

[6] J. Israelachvili, "Intermolecular and Surface Forces," *Academic Press* (1992).

[7] Dawn Bonnell, "Scanning Probe Microscopy and Spectroscopy : Theory, Techniques, and Applications," *John Wiley & Sons* (2000).